A linear least square approach for navigation using ultrasonic waves

Natee Thong-un[*1], Non-member

ABSTRACT

This paper presents a method to locate a moving object with velocities in three dimensional (3D) spaces by echolocation. This method can determine the object's position and velocity measurements, through computation from the original nonlinear model using a linear least square (LLS) - based approach. To satisfy the navigation problem and deal with the additive noise, Colored Gaussian Noise was considered as a performance parameter in computer simulations. The design system consisted of one loudspeaker and four acoustical microphones. An echo received from the microphone was converted into a one-bit stream, based on four channels, delta-sigma-modulation board. A field-programmable gate array (FPGA) was then applied to compute the recursive cross correlation, using one-bit signal processing. The object, considered as a flying ball, was positioned in 3D space at x-y-z coordinates. The dilution of precision and the uncertainty in the object position were also studied. The velocity of the object was calculated using a pair of linear-period-modulated ultrasonic signals. The validity was evaluated by the probability density function (PDF) and the cumulative density function (CDF) from repeated experimental results. The results of this proposed system using an LLS-based method can provide better repeatability, when compared against the linearization-based method.

Keywords: Linear-period-modulated ultrasonic signal, Linear-least-square, Position measurement, Velocity measurements, FPGA.

1. INTRODUCTION

Echolocation is a well-known method for determining obstacle positions by time-of-flight (TOF) computation from a reflector to a receiver. Bats possess the remarkable ability to sense the position of obstacles by generating a chirp signal at specific frequencies. The reflected echoes are then received and monitored by their ears. Bats use echolocation techniques to calculate their own position relative to objects [1,2] Echolocation can be useful in a variety of applications involving reflections, including non-destructive tests, medical systems, and, flow measurements, [3-5]. In addition, echolocation has been developed for a wide range of applications such as radar, sonar and ultrasonic [6-8]. Ultrasonic range measurement, an example of acoustic systems, has the significant advantages of acoustic sensors, small size, low cost, and uses simple hardware. It is a relatively flexible area for robotics requiring environmental navigation. However, the most critical disadvantage for robot navigation results from the determination of obstacles. Precise identification of an object's location is required to support the self-localization process. Advanced technology which relies on laser ranging is relatively expensive; moreover, this is not appropriate for real-time robot navigation, as lasers have very narrow beams compared with ultrasound for position determination in 3D spaces. In general, one dimensional object positioning, using an ultrasonic system can be easily achieved by multiplication of the sound velocity and the TOF. Cross correlation is a key idea to compute TOF because this has advantages compared with other methods for dealing with signal-processing problems at low signal-to-noise ratio (SNR) [9]. The cross correlation method has therefore been used extensively in ultrasonic ranging measurements [10, 11]. The principle of the cross correlation method is based on a number of lag products between an echo from an object, and a reference signal. The TOF of a received signal is typically estimated from the maximum peak time in the cross correlation function, and it is therefore a simple task to find any object location in an interesting condition. In the case of concurrent position and velocity measurements, the ambiguity function method used to determine these variables for the moving object is well known in radar technology. The delay time and the Doppler shift of a chirp signal are calculated by the cross ambiguity function. However, this technique requires fast Fourier transform (FFT) of the lag products, and has many multiplications and accumulations compared with the general cross correlation [12]. This paper, therefore, presents a method for concurrent position and velocity measurements without computations on the frequency domain, to satisfy real-time applications.

One-bit signal processing is a well-known technique used as a digital convertor of Super Audio CD (SACD), and ensures that SACD has higher audio quality than other techniques [13], because the quantization noises from analog to digital con-

Manuscript received on February 10, 2016 ; revised on February 15, 2016.

*The Department of Instrumentation and Electronics Engineering King Mongkut University of Technology North Bangkok, Thailand, Email : thnatee@yahoo.co.th[1]

version (ADC) can be decreased by delta-sigma modulation. Cross correlation with high resolution based on one-bit signal processing has been proposed for ultrasound [9]. This is an over-sampling low-computational-cost technique for TOF computation, using a linear-frequency-modulated (LFM) signal. However, a significant problem of LFM signals is that they cannot completely correlate with an echo reflected from a moving object due to the Doppler effect. To overcome this, a linear-period-modulated (LPM) signal was presented, rather than a LFM signal for ultrasonic systems [14]. The method of applying LPM signals provided the cross-correlation functionality to achieve the TOF, but the time consumption problem was an important issue for real-time applications. Accordingly, a low cost, high resolution ultrasonic system, involving distance measurements using pulse compression with two cycles of LPM signals and Doppler-shift compensation was suggested [15]. This paper developed these earlier ideas to present a novel ultrasonic position measurement technique, based on the recursive cross-correlation method embedded on a field-programmable gate array (FPGA), and the velocity measurement from a pair of LPM ultrasonic waves including Doppler-shift compensation. The moving object position was located as x-y-z coordinates by the linear least square (LLS)-based method. The validity of the proposed method was guaranteed by computer simulations and the experimental results.

2. PROPOSED POSITION AND VELOCITY MEASUREMENTS

The ultrasonic system proposed in this paper is depicted in Fig. 1. The devices used consisted of a loudspeaker and four acoustical receivers. A transmitted signal to the speaker was composed using couple of two LPM ultrasonic signals. An echo signal from the flying object was received by the microphone. The echo was changed into one-bit stream signals by four delta-sigma modulators. A digital comparator was used as a reference signal for conversion. Both the one-bit stream signals were then processed together to achieve TOF, using the cross-correlation method according to Fig. 1. The first couple peaks were recorded directly from the loudspeaker, and the second couple peaks were recorded on the microphones. The length of signals l_0 and l_d were used for velocity measurement calculation.

2.1 Position measurements

The proposed system (Fig. 1) measured the position of a flying object, with ranging measurements from the -X to +X axis, and from the -Z to +Z axis. The object was set on only +Y axis. The first, second, third, and fourth microphones were placed on the X and Z axes. Their locations were (x_1,0,0), (x_2,0,0), (0,0,z_3), and (0,0,z_4). The object was assumed as an

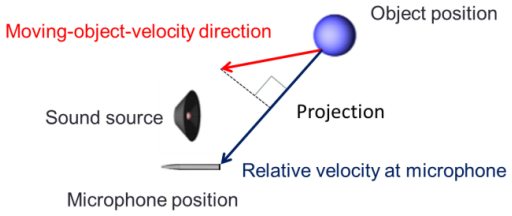

Fig.2: *Velocity vector measurement.*

unknown parameter (x, y, z). The distance from the loudspeaker position to the object was d. The relation of the microphone position, the object position, and the TOFs was:

$$d + \sqrt{(x - x_1)^2 + y^2 + z^2} = v_{sound} TOF_1 \quad (1)$$

$$d + \sqrt{(x - x_2)^2 + y^2 + z^2} = v_{sound} TOF_2 \quad (2)$$

$$d + \sqrt{x^2 + y^2 + (z - z_3)^2} = v_{sound} TOF_3 \quad (3)$$

$$d + \sqrt{x^2 + y^2 + (z - z_4)^2} = v_{sound} TOF_4 \quad (4)$$

where TOF_i is the time-of-flight at each microphone position, and i = 1, 2, 3 and 4, respectively. TOF was computed based on the cross-correlation function. The four nonlinear equations (1) - (4) were converted into a linear form and expressed as:

$$2\mathbf{A} \cdot \mathbf{b} = \mathbf{c} \quad (5)$$

v_{sound} is the velocity of sound. Thus, an unknown vector $\mathbf{b}$ was estimated by the LLS-based method as Eq.(6), where

$$\mathbf{A} = \begin{bmatrix} -x_1 & 0 & v_{sound} TOF_1 \\ -x_2 & 0 & v_{sound} TOF_2 \\ 0 & -z_3 & v_{sound} TOF_3 \\ 0 & -z_3 & v_{sound} TOF \end{bmatrix}, \mathbf{b} = \begin{bmatrix} x \\ z \\ d \end{bmatrix}$$

and $$\mathbf{c} = \begin{bmatrix} -x_1^2 + v_{sound}^2 TOF_1^2 \\ -x_2^2 + v_{sound}^2 TOF_2^2 \\ -z_3^2 + v_{sound}^2 TOF_3^2 \\ -z_4^2 + v_{sound}^2 TOF_4^2 \end{bmatrix}$$

$$\mathbf{b} = \frac{1}{2} \left(\mathbf{A}^T \mathbf{A} \right)^{-1} \mathbf{A}^T \mathbf{c} \quad (6)$$

Finally, y was computed as $y = \sqrt{d^2 - x^2 - z^2}$.

2.2 Velocity measurements

The relative velocity measurements (v_d), the instantaneous position of the moving object, and the microphone positions were all key ideas for estimation. The relative velocity was estimated by the duration between the first peak and the second peak as (Fig. 1). The relative velocity is defined in Eq. (7).

$$v_d = \frac{l_0 - l_d}{l_0 + l_d} v_{sound} \quad (7)$$

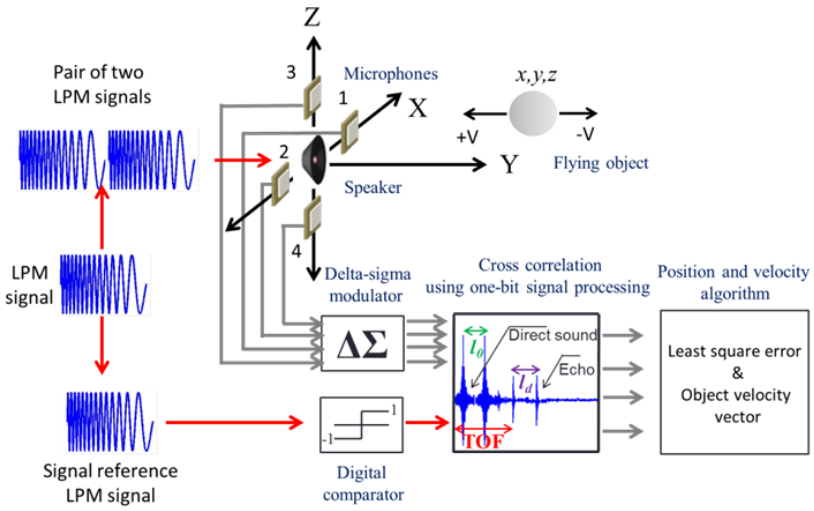

Fig. 1: *Proposed position and velocity measurements based on the recursive cross correlation.*

Vector projection relied on the fundamentals of three-dimensional Doppler velocimetry [16]. The dot product between the two vectors is shown in Fig. 2. An unknown vector of the moving object, based on x-y-z coordinates was expressed as $\mathbf{u} = [u_x, u_y, u_z]^T$, and the relative velocities at microphones 1, 2, 3, and 4 were $v_d = [v_{d1}, v_{d2}, v_{d3}, v_{d4}]^T$. Then, the definition of the vector projection is:

$$\mathbf{v}_d = [\frac{\mathbf{u}^T \cdot \mathbf{p}_1}{\|\mathbf{p}_1\|}, \frac{\mathbf{u}^T \cdot \mathbf{p}_2}{\|\mathbf{p}_2\|}, \frac{\mathbf{u}^T \cdot \mathbf{p}_3}{\|\mathbf{p}_3\|}, \frac{\mathbf{u}^T \cdot \mathbf{p}_4}{\|\mathbf{p}_4\|}]^T \qquad (8)$$

where $\mathbf{p}_1 = [x_1 - x, -y, -z]^T$, $\mathbf{p}_2 = [-x_2 - x, -y, -z]^T$, $\mathbf{p}_3 = [-x, -y, z_3 - z]^T$, and $\mathbf{p}_4 = [-x, -y, -z_4 - z]^T$. These are all directions from the instantaneous position of the moving object to the microphone positions. Again, the vector $\mathbf{u}$ based on the LLS estimate can be expressed as:

$$\mathbf{u} = \left(\mathbf{H^T H}\right)^{-1} \mathbf{H^T W g} \qquad (9)$$

where

$$\mathbf{H} = -\begin{bmatrix} x-n & y & z \\ x+n & y & z \\ x & y & z-m \\ x & y & z+m \end{bmatrix}, \mathbf{W} = \frac{1}{4}\begin{bmatrix} 1 & 1 & 1 & 1 \\ 1 & 1 & 1 & 1 \\ 1 & 1 & 1 & 1 \\ 1 & 1 & 1 & 1 \end{bmatrix}$$

and $\mathbf{g} = [v_{d1} \cdot \|\mathbf{p}_1\|, v_{d2} \cdot \|\mathbf{p}_2\|, v_{d3} \cdot \|\mathbf{p}_3\|, v_{d4} \cdot \|\mathbf{p}_4\|]^T$ The weighted averaging matrix W was then placed into Eq. (9) to stabilize the variance of the relative velocity in all microphones.

3. EVALUATION OF THE PROPOSED METHOD BY COMPUTER SIMULATION

The moving object position under the proposed system, determined by one-bit signal processing was evaluated by MATLAB computer simulations. Assuming that the period of LPM signal varied linearly from 20 μs to 50 μs, the length of a pair of LPM signals was 6.548 ms. The sampling frequency rate was 12.5 MHz. The microphone coordinates were (10,0,0), (-10,0,0), (0,0,10), and (0,0,-10) cm. The propagation velocity of an ultrasonic wave in air was 345.1 m/s at 22.4 °C. The attenuation in air was approximately 2.11 dB/m [17]. The smoothing operation in the cross-correlation function was accomplished by the 141- tap triangular weighted moving average filter. The object shape was assumed as a very small point.

3.1 Position error due to Colored Gaussian Noise

This paper presented a proposed system to deal with navigation problems in the fields of radar or sonar involving Color Gaussian Noise [18, 19]. To continue further, it is necessary to provide some background information on the nature of Colored Gaussian Noise. A particularly useful model for Colored Gaussian Noise is the autoregressive (AR) model. This takes the mathematical form with the non-flat power signal density (PSD) as:

$$P(f) = \frac{\sigma^2}{|1 + a\,[1] \exp(-j2\pi f) + ...a\,[p] \exp(-j2\pi f)|^2} \qquad (10)$$

where σ^2 is a variance of random signals. The model order was realized in the definition by referring to it as an AR (p) of the PSD model. Its usefulness is relied on PSD, as long as the model order p was chosen large enough. This paper considered the AR (1) model given by:

$$P(f) = \frac{\sigma^2}{|1 + a\,[1] \exp(-j2\pi f)|^2}. \qquad (11)$$

For a [1] = -0.5 and σ^2 = 3, Colored Gaussian Noise is shown in Fig. 3. Colored Gaussian Noise as previously explained was added to the LPM signals to

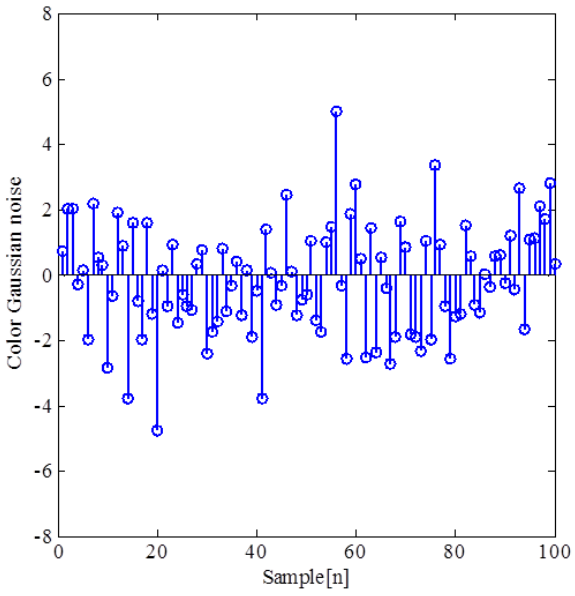

Fig.3: *Realization of Colored Gaussian Noise with AR (1) model: a [1] = -0.5 and σ^2 = 3.*

account for noise effects with SNR of 10 and 0 dB. For each SNR, the position of the object was estimated from 100 simulations. The probability distributions of the estimated positions are illustrated in Fig. 4 and Fig. 5 for SNRs of 10 dB and 0 dB, respectively. Precisions of x-position, y-position, and z-position are 35.0337 ± 0.0876 cm, 65.0561 ± 0.0715 cm, and 25.0308 ± 0.0854 cm, respectively. Based on simulations, the precision of the proposed method was less than 0.1 cm for all unknown parameters.

3.2 Comparison with other methods

The LLS estimate - based method improved from the nonlinear equations was realized: normally they can be solved directly by iterative methods [20]. An earlier work by the authors of this paper involved with the position measurement relied on linearization and was presented using three microphones [21]. To assess the performance of the proposed system, a comparison was made with the former methods by varying a distance from x = 35 to 36 cm, y = 65 to 66 cm, and z = 25 to 26 cm with SNR of 0 dB. As shown in Fig. 6, the Newton-Raphson method, the linearization - based method, and the LLS estimate - based method have similar accuracy; they are all relatively close to the reference line. For the LLS - based method, the accuracy of the x-position was lower than 0.5 mm, the y-position was lower than 1 mm, and the z-position was approximately 0.5 mm.

3.3 Position dilution of precision (PDOP)

The study of PDOP involved searching out the appropriate evaluation units to provide a better geometric configuration and estimation. PDOP relates to the uncertainty in the object position (x, y, z) regarding the distance (d). This parameter defined a ratio of errors, directly affecting the object position when the distance was varied. With a smaller PDOP, the proposed method becomes less sensitive to error [22]. Basically, the PDOP

$$PDOP = \frac{\sqrt{\sigma_x^2 + \sigma_y^2 + \sigma_z^2}}{\sigma_d} \tag{12}$$

can be defined as Eq. (12), where σ_x, σ_y, and σ_z are the standard deviations of the object position, and σ_d relates to the distance. Simulation results as shown in Fig. 7 explain that at the same y-coordinate, when the object position was pushed further away from a central point, errors on the x-z plane became more sensitive. The results implied that with increasing distance the object became, more sensitive to errors in position.

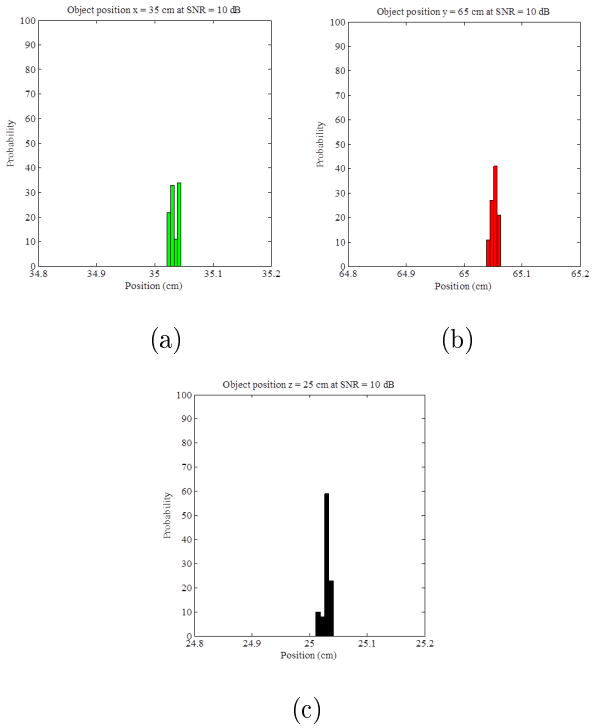

(a) (b)

(c)

Fig.4: *The probability distributions of the estimated position in the simulations at SNR = 10 dB from the cross-correlation function (a) x-position (b) y-position and (c) z-position.*

3.4 Effect of microphone positions to accuracy

The proposed equations, Eq. (1) - (4) show that, the position of the object is also derived from the microphone positions on the X and Z axes. The accuracy of the LLS method was investigated by varying

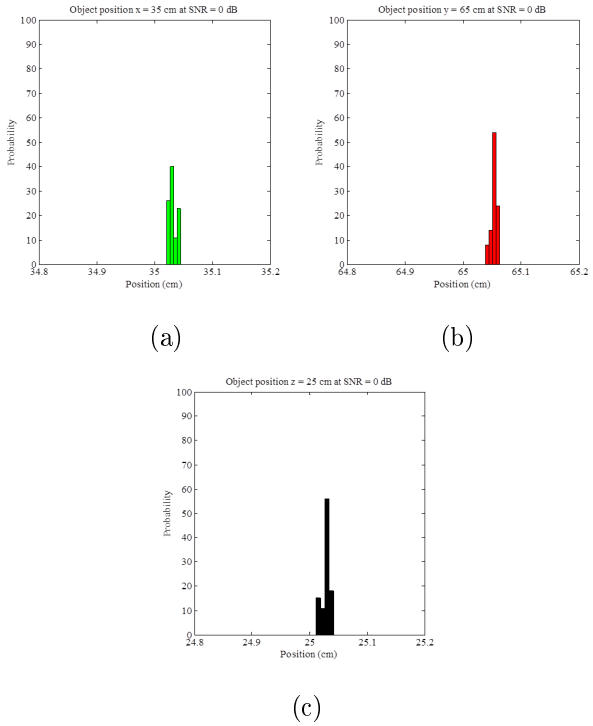

Fig.5: *The probability distributions of the estimated position in the simulations at SNR = 0 dB from the cross-correlation function (a) x-position (b) y-position and (c) z-position.*

the microphone positions, while keeping the object position unchanged. The microphone pattern was re-arranged according to Fig.8. The first and second microphones were moved to +X and -X, and the third and fourth microphones were varied along +Z and -Z. Then, each microphone position was varied by the same value, in each line from 0 to 50 cm. Simulation results revealed that the object position showed high variance when the microphone positions were changed from 0 to about 10 cm (Fig.9 (a) - (c)). However, when the microphone passed through 10 cm, the object position became more stable. Therefore, the microphone position for the experimental setup was established at least 10 cm distant from the speaker location. This optimal location for the microphones was then used in the experimental study as illustrated in Fig. 10.

4. EXPERIMENTAL PROCEDURE

4.1 Experimental setup

The experimental setup to support the LLS estimate-based method is shown in Fig. 10. In the experiment, the frequency of a pair of transmitted LPM signals was down chirp tuned from 50 to 20 kHz. The length of the LPM signal was 3.274 ms. The driving voltage of the signal generator was 4 Vp-p, and enlarged 10 times using an amplifier. The loudspeaker used was a Pioneer PT-R4. The spherical object target had a diameter of 10 cm. Moreover, the echo

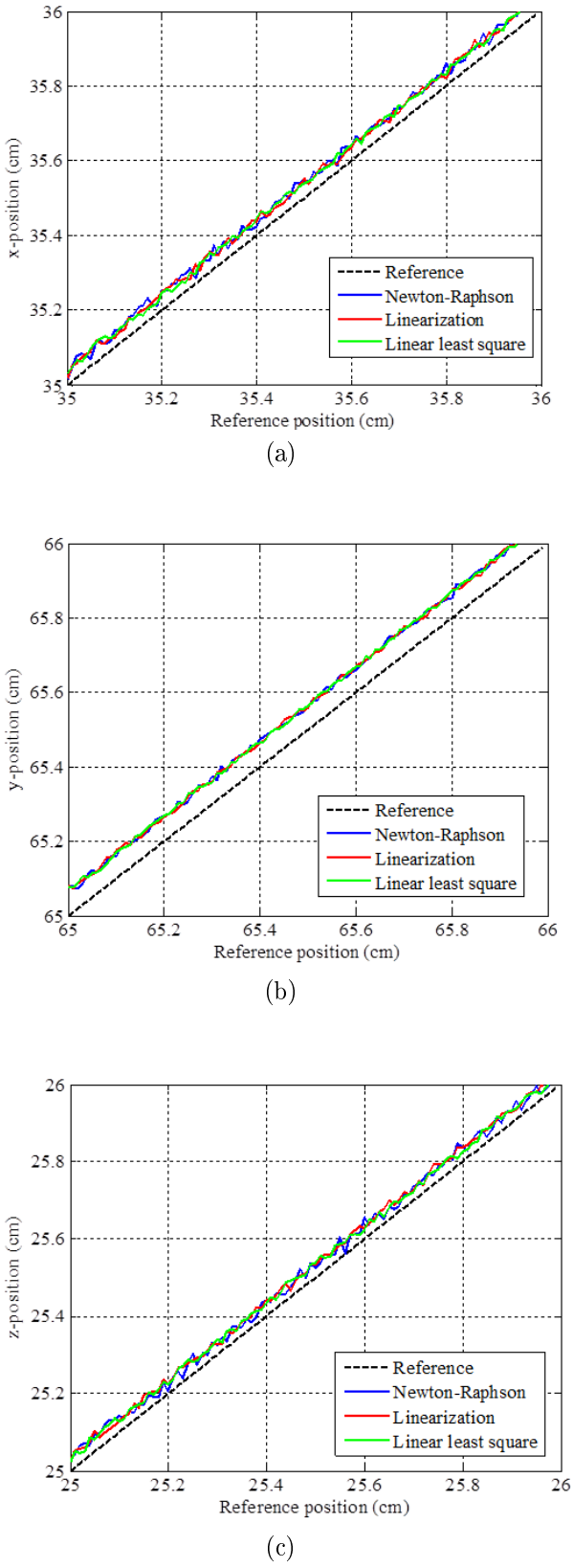

Fig.6: *Compare of accuracy between the Newton-Raphson, the linearization, and the LLS: (a) x-position, (b) y-position, and (c) z-position.*

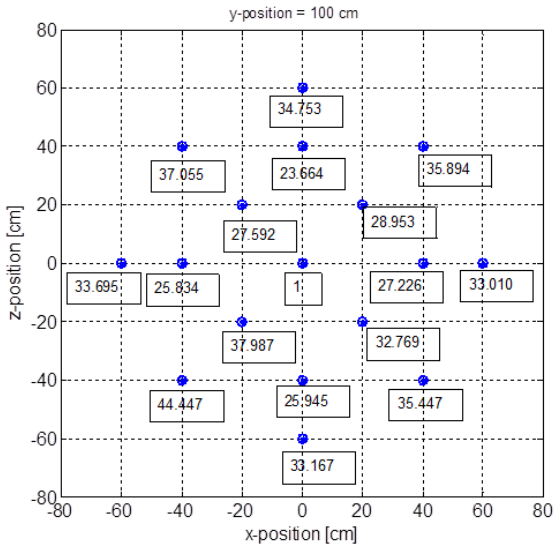

Fig. 7: *PDOP in the x-z plane at y = 1 m from the original point.*

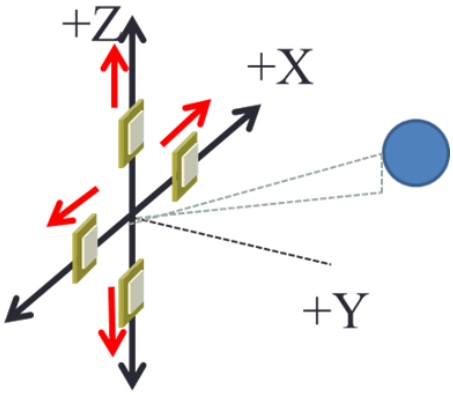

Fig. 8: *The direction of varying microphone positions.*

sensed by the four silicon MEMS microphones relied on a device for hand-held telecommunication instruments (Knowles SPM024UD5). This device was embedded on a signal processing board, having a low-pass frequency circuit, with 60 kHz frequency cutoff and a pre-amplifier with 20 dB. Sensitivity was set at a minimum level of -47 dB. Each microphone position was set at a distance of 10 cm on the X and Z axes, far away the original point. The propagation velocity for LPM signals was approximately 345 m/s. The echoes sensed by the microphones were changed into one-bit signals by 7^{th}-order delta-sigma modulator (Analog Devices AD7720). The sampling rate of the delta-sigma modulator was 12.5 MHz. The cross correlation and smoothing operation with 144 taps of a weighted moving average filter was programmed into a FPGA board model cyclone V 5CGXFC5C6F27C7.

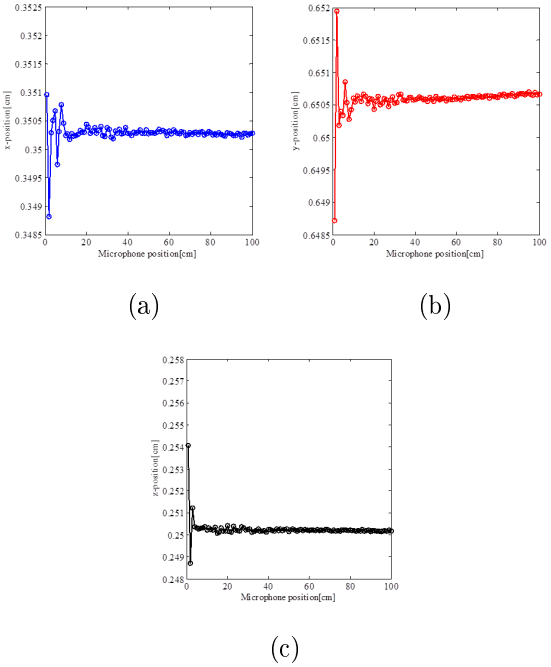

Fig. 9: *Accuracy when changing microphone positions at the object position x = 35 cm, y = 65 cm, z = 25 cm (a) x-coordinate error, (b) y-coordinate error, and (c) z-coordinate error.*

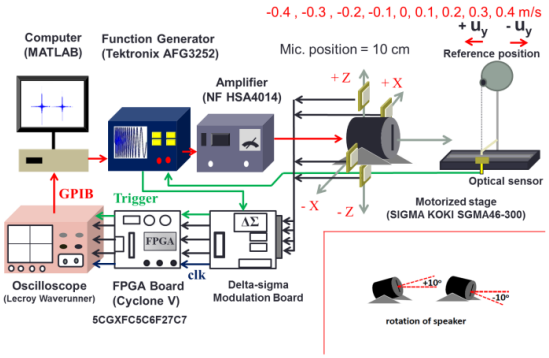

Fig. 10: *Experimental setup of ultrasonic position and velocity measurements based on the LLS method.*

The total logic of the FPGA board for the cross correlation computation designed to support one-bit signal processing was 2602 logic elements; the total number of registers was 5777, and the total block memory involved was 175,948 bits. The object was driven using a SIGMA KOKI SGMA46-300 motorized stage in only the +Y and -Y direction, with a maximum and minimum speed of ±0.4 m/s. The velocity was adjusted by ± 0.1 m/s at each step. To satisfy the ability of the sound-beam radiation to cover an object position, the ball was positioned on the left- and right-hand sides, away from the sound-beam radiation source.

4.2 Position measurements of a stationary object

The position of the stationary object was repeated for 50 experiments; the probability distributions of the measured position are illustrated in Fig. 11. The object location measurements are depicted by the different color bars. The reference points of the blue bar, the green bar, the red bar, the black bar, and the pink bar were (0, 84, 27), (26, 69, 4), (-43, 63, 13), (30, 43, -17), and (-41, 53, -31) cm, respectively. The experimental results showed that the object position, x = 0 cm, y = 84 cm, and z = 27 cm, had the minimum variance. This can be explained because the position was established near the central line of the +Y axis of sound shown as (Fig. 1). The sound pressure moved toward the target and then returned to the receivers with intense sound pressure. The variance of the point of contact on the surface was low. On the other hand, when the target was in the other positions, maximum dispersion of repeatability was noticed, since these locations were positions relatively far away from the main sound beam, and therefore, the repeatability of contact at the same place was less likely.

4.3 Position measurements of a moving object

The position measurement was determined at different velocities from the maximum point to the minimum point, according to the performance of the motorized stage. Fifty experiments were recorded at each position of the moving object driven by the motorized stage. The positions with different velocities were evaluated using the cumulative density functions (CDFs), (Figs. 12 - 13). The first reference position was assumed to be x = 20 cm, y = 94 cm, z = 7 cm, and the second was x = 23 cm, y = 68 cm, z = -30 cm. The position and velocity of the determined moving object were measured concurrently by the proposed method, based on one-bit signal technology. For the experimental results at the first reference point near the x-y plane (x = 20 cm, y = 94 cm, z = 7 cm), the maximum position errors were approximately 0 - 2 cm for all x, y, and z parameters. Next, the moving object position was considered to have a location far away from the x-y plane at (x = 23 cm, y = 68 cm, z = -30 cm). The experimental result at this position showed an error interval at 0-3 cm. The errors at this location were larger than at the former position of about 1 cm. Thus, as the object position moved further from the x-y plane, the error in the position also increased. In practice however, the deviations between the assumed reference position and the measured position observed from the experimental results were probably caused by the moving object used in this paper, which was a rigid body, while the object computed from the proposed method was assumed to be a very small point. Accordingly, the sound beam moving toward the moving object, and incident on

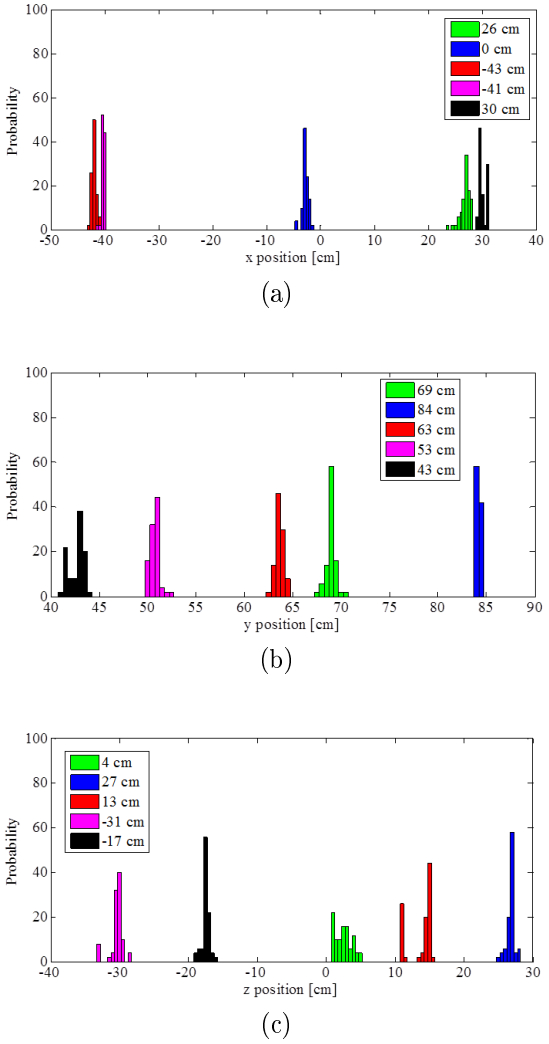

Fig. 11: *Probability of the position of the stationary object: (a) x position, (b) y position, and (c) z position.*

the surface was propagated from many points, which then resulted in many different TOFs at the microphone [21]. This noticeably affected the efficiency, producing an uncertainty due to the variance of the proposed position and velocity measurements.

4.4 Velocity measurements of a moving object

Fig. 14 shows the velocity measurement determined in the ± Y direction (u_y) in the probability density function (PDF), in the same direction of the motorized stage movement. The component vectors of u_x and u_z were determined at close to zero. The velocity measurement results for the first position are shown as Fig. 14 (a). The accuracy of the u_y velocity component for the first case agreed with the reference. The velocity measurement results for the second case are shown as Fig. 14 (b). The accuracy of the u_y velocity component for the second case was smaller than the reference by about ±0.05 m/s for the higher

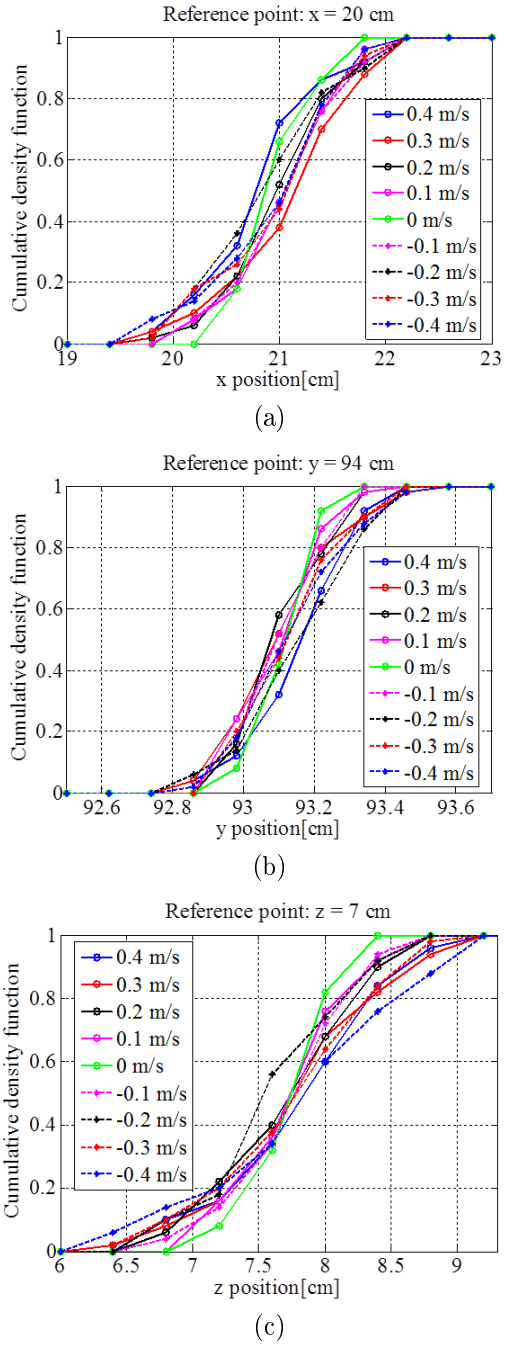

Fig.12: *Cumulative density function of position error at x = 20 cm, y = 94 cm, and z = 7 cm when varying the velocity (a) x-position, (b) y-position, and (c) z-position.*

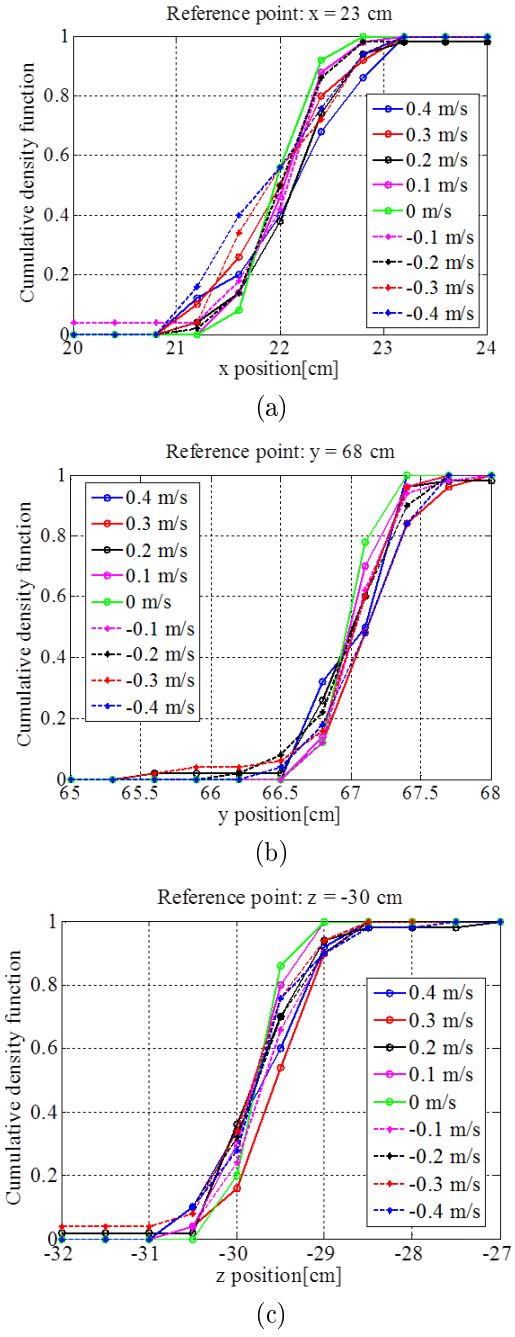

Fig.13: *Cumulative density function of position error at x = 23 cm, y = 68 cm, and z = -30 cm when varying the velocity (a) x-position, (b) y-position, and (c) z-position.*

velocity ±0.4 m/s. The deviations of measurement can be explained as a rod connecting the object and the motorized stage, and swung with higher vibration when the moving object was accelerated to the maximum velocity in each turn. Therefore, the moving object did not completely stop, and was not at a static condition during the next measurements [21]. The higher vibration velocity on surface, due to the moving object, strongly affects to the repeatability.

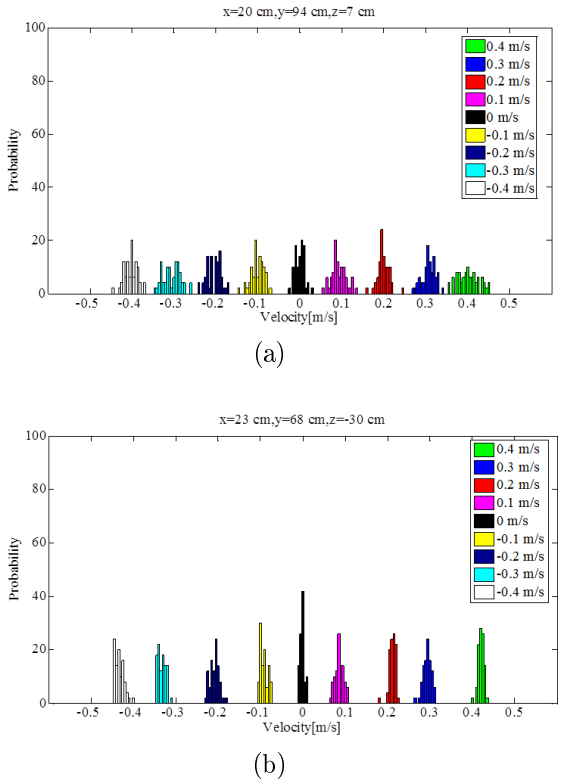

Fig.14: *Probability density function of velocity measurement: (a) first position, and (b) second position.*

5. CONCLUSIONS

This paper presented an optimal method of concurrent position and velocity measurement that relied on the LLS estimate - based method. The proposed method consisted of one-bit signal processing for TOF computation with low-computation costs. The object position was assumed as x-y-z coordinates. The accuracy of the proposed method was verified by simulation under Colored Gaussian Noise. The positions measured in this system were determined by 50 experiments for each position. The maximum error was determined at about 0.3 cm for a sound velocity of 345 m/s, and an oversampling rate of 12.5 MHz. The results indicated that a position considered near the central line of the sound beam and the x-y plane achieved the lowest variance of repeatability. In addition, the deviation in the actual results occurred because the object was assumed to be a very small point, but in reality, a spherical object was used as the rigid body object. The exact position of the reference point on the surface that the sound beam approached was not known. Thus, the sound beam might not be incident on the assumed reference point. This was a possible reason for deviations from the measurements. Moreover, the vibration on the surface of the moving object directly affected the velocity measurements. However, the results of the proposed system using the LLS-based method can locate the obstacle with the higher repeatability compared with the linearization-based method [21].

References

[1] S. P. Dear, J. A. Simmons, and J. Fritz, "A possible neural basis for representation of acoustic scenes in auditory cortex of the big brown bat,"*international weekly j. of science*, pp. 620-623, 1993.

[2] M. Yano, I. Matsuo, and J. Tani, "Echolocation of multiple target in 3-D space from a single emission,"*J. of Biological Physics*,Vol.28, no. 3, pp. 509-525, Sep. 2002.

[3] W. Padungsriborworn, A. Furukawa, and S. Hirose, "Improvement of SAFT by Implementation of Approximate Wave Solution in Fluid-Solid Two-Phase: A Case Study on Imaging of Aluminum Rod with Side-Drilled Holes," *J. of Nondestructive Eval.*, 2015, pp. 1573-4862.

[4] S. Wada, K. Tezuka, W. Treenuson, N. Tsuzuki, and H. Kikura, "Study on the optimal Number of Transducers for Pipe Flow Rate Measurement Downstream of a Single Elbow Using the Ultrasonic Velocity Profile Method," *Science and Technology of Nuclear Installations*, vol. 2012, pp. 1-12 , Jun. 2012.

[5] A. Trucco, S. Curletto, and M. Palmese, "Interpolation of Medical Ultrasound Images From Coherent and Noncoherent Signals," *IEEE Transactions on Instrumentation and Measurement*, vol. 58, no. 7, pp. 2048 - 2060, Jul. 2009.

[6] L. J. Stankovic, T. Thayaparan, and M. Dakovic, "Signal Decomposition by Using the S-Method with Application to the Analysis of HF Radar Signals in Sea-Clutte," *IEEE Transactions on Signal Processing*, vol. 54, no. 11, pp. 4332 - 4342, Nov. 2006.

[7] Z.-J Yao, Q-H. Meng, and M. Zeng, "Improvement in the accuracy of estimating the time-of-flight in an ultrasonic ranging system using multiple square-root unscented Kalman filters," *Sci. Instrum.*, vol. 81, no. 10, Oct. 2010.

[8] T. Schlegl, T. Bretterklieber, M. Neumayer, and H. Zangle, "Combined Capacitive and Ultrasonic Distance Measurement for Automotive Applications," *IEEE Sensors J.*, vol. 11, no. 11, pp. 2636 - 2642, Nov. 2011.

[9] S. Hirata, M. Kurosawa, and T. Katari, "Accuracy and resolution of ultrasonic distance measurement with high-time-resolution cross-correlation function obtained by single-bit signal processing," *The Acoustical Society of Japan*, vol. 30, no. 6, pp. 429-438, Jan. 2009.

[10] R. Queiros, P. S. Girao, and A. C. Serra, "Cross-Correlation and Sine-Fitting Techniques for High-Resolution Ultrasonic Ranging," *Instrumentation and Measurement Technology Conf.*, Sorrento, Italy, 2006, pp 552 - 556.

[11] M. M. Saad, C. J. Bleakley, and S. Dobson, "Ro-

bust High-Accuracy Ultrasonic Range Measurement System," *IEEE Transactions on Instrumentation and Measurement*, vol. 60, no. 10, pp. 3334 - 3341, Oct. 2011.

[12] L. Christopher, "Computing the cross ambiguity function âĂŞ A review," Master Thesis, Binghamton University, State University of New York, 2001.

[13] Super Audio CD, "Production Using Direct Stream Digital Technology," *Electronics and Sony Corporation copyright*, http://www.canadapromedia.com

[14] J. J. Kroszczynski , "Pulse compression by means of linear-period-modulated," *Proceedings of the IEEE*, vol. 57, no. 7, pp. 1260 - 1266, Jul. 1969.

[15] S. Hirata, and M. K. Kurosawa, "Ultrasonic distance and velocity measurement using a pair of LPM signals for cross-correlation method improvement of Doppler-shift compensation of Doppler velocity estimation," *Ultrasonics*, vol. 52, no. 7, pp. 873âĂŞ879, Sep. 2012.

[16] M. D. Fox and, W. M. Gardiner, "Three-dimensional Doppler velocity of flow jet," *IEEE Transactions on Biomedical Engineering*, vol. 35, no. 10, pp. 834 - 841, Oct. 1988.

[17] E. J. Evans, and E. N. Bazley, "The absorption of sound in air at audio frequencies," *Acoustica 6*, 1956, pp. 238-245.

[18] F. E. Nathanson, "Radar Design Principles," *SciTech Pubs. New York*, 1999.

[19] W. S. Burdic, "Underwater Acoustic Systems Analysis," Prentice-Hall, Englewood Cliffs, New Jersey, 1984.

[20] K. P. Chong and, S. H. Zak, "Introduction to optimization," John Wiley & Sons, Inc., New York, 2001.

[21] N. Thong-un, S. Hirata, Y.Orino, and M. K. Kurosawa, "A linearization-based method of simultaneous position and velocity measurement using ultrasonic waves," *Sensors and Actuators A: Physical*, vol. 266, no. 1, pp. 480 - 499, Sep. 2015.

[22] A.J. Martin, A.H. Alonso, D. Ruiz, I. Gude, C.D. Marziani M.C. Perez, F.J. Alvarez, C. Gutierrez, and J. Urena, "EMFi-based ultrasonic sensory array for 3D localization of reflectors using positioning algorithm," *IEEE Sensors J.*, vol. 15, no. 5, pp. 2951 - 2962, May. 2015.

Natee Thong-un was born in Samutprakarn, Thailand. He received the B.Eng. degree in Instrumentation system engineering from King Mongkut Institute of Technology North Bangkok, Thailand, in 2004. He received the M.Eng. Degree in Instrumentation Engineering from King Mongkut Institute of Technology Ladkrabang, Thailand, in 2006. He received his D.Eng. Degree in Information Processing from Tokyo Institute of Technology, Japan, in 2015. Since 2016, he has been a lecturer in the Department of Instrumentation and Electronics Engineering, King Mongkut University of Technology North Bangkok. His current research interests include measurement using airborne ultrasound, flow measurement based on ultrasonic wave, ultrasonic nondestructive evaluation, numerical analysis of ultrasonic propagation, and statistical signal processing for ultrasound. Moreover, he is a member of the Acoustical Society of Japan, and IEEE.